

Spin-Up from Rest in a Differentially Rotating Cylinder

Jae Min Hyun*

Clarkson College of Technology, Potsdam, New York

Spin-up from rest in a cylinder with top and bottom end-wall disks rotating at different rates (Ω_T and Ω_B , respectively) is investigated by numerically integrating the unsteady Navier-Stokes equations. The approximate analytical model due to Wedemeyer and Venezian is briefly recounted. Numerical solutions for three sets of Ω_T/Ω_B for a cylinder of aspect ratio $\mathcal{O}(1)$ and a minute Ekman number are presented. The results are detailed flowfield data that display the transient azimuthal velocity profiles, axial vorticity distributions, and the meridional flow patterns. An azimuthal velocity shear front, which separates the rotating from the nonrotating fluid, propagates radially inward. As Ω_T/Ω_B becomes close to unity, the propagation speed of the front increases and the spin-up in the interior is more effective. The axial vorticity is zero ahead of the front and is larger than twice the final-state angular speed of the fluid behind the front. The meridional circulation is no longer antisymmetric about the cylinder mid-depth as Ω_T/Ω_B deviates from unity. The final-state meridional circulation in the interior consists of purely vertical flows pulled toward the faster rotating end-wall disk. At early times, in a manner similar to spin-up in a rigid cylinder, the interior fluid is drawn into the end-wall Ekman layers ahead of the front and blown out of the Ekman layers behind the front. At large times, however, the faster rotating disk sucks in the interior fluid behind as well as ahead of the front.

Introduction

CONSIDER a closed right rigid cylinder of radius a and height H filled with an incompressible fluid of kinematic viscosity ν . Both the container and the fluid are initially at rest. At time $t=0$ the cylinder is impulsively started spinning about the cylinder axis at a rotation rate Ω , which is subsequently maintained constant. The transient adjustment process of the fluid to the rotating container is referred to as "spin-up from rest." Knowledge of this internal flow is needed to design spin-stabilized liquid-filled projectiles and rockets.¹⁻³ Spin-up from rest has been the subject of extensive investigations (e.g., Refs. 1-10); in particular, recent work of Kitchens^{1,2} and Hyun et al.¹⁰ presented numerical solutions of the governing Navier-Stokes equations. We assume here that the cylinder aspect ratio a/H is $\mathcal{O}(1)$ and that the Ekman number $E=\nu/\Omega H^2$ is very small [$\mathcal{O}(10^{-4})$ in this paper]. Thus, we are concerned with fluid motions in which the Coriolis force will be an essential ingredient in the balance of forces. It has been established that the most important process controlling spin-up is the weak meridional circulation driven by Ekman layers on the end-wall disks. Therefore, the fluid adjustment is substantially accomplished in the spin-up time scale $\mathcal{O}(E^{-1/2}\Omega^{-1})$.

The present paper deals with the problem of spin-up from rest in a differentially rotating cylinder, i.e., the top end-wall disk rotates at Ω_T , the bottom disk at Ω_B , and the sidewall at Ω_S . Although the principal mechanism of the meridional circulation driven by the Ekman layers is still predominant, there are some important differences between this flow and the spin-up in a rigid cylinder. First, unlike the case of a rigid cylinder, the final state of this flow is not strictly a solid-body rotation. In the final state, there is a meridional circulation induced by the Ekman suction (blowing) of the interior fluid at the faster (slower) rotating disk throughout its length. Therefore, the transient meridional flows evolve from the initial state of rest to a steady final-state circulation. The azimuthal flow is similar to that in a rigid cylinder; a velocity shear front propagates radially inward, dividing the transient azimuthal flow into two regions. The final-state angular speed of the interior fluid takes a value between Ω_T and Ω_B .

A highly approximate analytical model for spin-up from rest in a differentially rotating cylinder was formulated by Venezian¹¹ that is a direct application of Wedemeyer's⁴ model for spin-up in a rigid cylinder. According to the Venezian model, the transient flows in a differentially rotating cylinder are approximately equivalent to those arising in a rigid cylinder if an appropriately defined angular speed Ω , which is a function of Ω_T and Ω_B , is used for the spin-up in a rigid cylinder. Venezian's model has been the major contribution in capturing the qualitative essentials of the flow.

The purpose of this work is to present accurate and comprehensive flowfield pictures for spin-up from rest in a differentially rotating cylinder. We present herein the results of numerical integrations of the unsteady Navier-Stokes equations using the numerical technique of Warn-Varnas et al.¹² The numerical solutions enabled us to examine details of the flow that cannot be readily obtained by laboratory measurements. These numerically generated, accurate flowfield data will also shed light on the limitations of the analytical model due to Wedemeyer and Venezian. The main results will be in 1) the transient azimuthal velocity profiles, 2) the axial vorticity distributions, 3) the patterns of the transient meridional circulation, and 4) the vertical velocity profiles. Of particular interest is the dependency of the transient flows on the parameter Ω_T/Ω_B , which was not explicitly accounted for in the Venezian model.

Analytical Model

In this section, we shall briefly recount the analytical model due to Wedemeyer⁴ and Venezian.¹¹ Let (r, θ, z) denote the cylindrical coordinates in an inertial frame of reference and (u, v, w) the corresponding velocity components. We take the mid-depth plane at $z=0$ so that the fluid is confined in $0 \leq r \leq a$ and $-H/2 \leq z \leq H/2$.

The fundamental theoretical model for spin-up from rest in a rigid cylinder was proposed by Wedemeyer.⁴ By a scaling argument, Wedemeyer took u , w , and $1/3 v / 1/3 z$ to be small in the interior. Furthermore, by assuming a linear relation between u and v through the Ekman compatibility condition, $u=f(v)$, he derived an equation for v in the interior

$$\frac{\partial V}{\partial T} + (V-R) \left(\frac{\partial V}{\partial R} + \frac{V}{R} \right) = A^{-2} E^{1/2} \left[\frac{\partial^2 V}{\partial R^2} + \frac{\partial}{\partial R} \left(\frac{V}{R} \right) \right] \quad (1)$$

Received July 23, 1982. Copyright © American Institute of Aeronautics and Astronautics, Inc., 1982. All rights reserved.

*Associate Professor, Department of Mechanical Engineering.

which is referred to as Wedemeyer's equation. The non-dimensional quantities, which appear in Eq. (1) and elsewhere, are defined as $R=r/a$, $V=v/a\Omega$, $A=a/H$, $Z=z/H$, and $T=E^{1/2}\Omega t$, where t is time and Ω the rotation rate of the cylinder.

In the limit $A^{-2}E^{1/2} \ll 1$, so that the right side of Eq. (1) can be neglected, Wedemeyer found an analytic solution,

$$V=0 \quad \text{for } R \leq e^{-T}$$

$$= (Re^{2T} - R^{-1}) / (e^{2T} - 1) \quad \text{for } R \geq e^{-T} \quad (2)$$

The Wedemeyer inviscid solution [Eq. (2)] clearly indicates that the interior flow is divided into two regions by a moving front located at $R=e^{-T}$. The fluid in the region ahead of the front ($R \leq e^{-T}$) is nonrotating and the fluid behind the front ($R \geq e^{-T}$) is being spun up. The corresponding meridional flow can be computed by substituting Eq. (2) into the assumed $u=f(v)$ relation and using the continuity equation.

A direct extension of the Wedemeyer model to spin-up from rest in a differentially rotating cylinder was made by Venezian.¹¹ Venezian showed that the transient azimuthal flows in a differentially rotating cylinder are approximately the same as those in a rigid cylinder rotating at the final-state angular velocity Ω , which takes a value between Ω_T and Ω_B . Specifically, Venezian chose the expression $\Omega = [(\Omega_B^2 + \Omega_T^2)/2]^{1/2}$, which was facilitated by the numerical data¹³ calculated for the steady-state flow between two infinite plates rotating at different rates. However, it should be noted that the transient vertical velocity in a differentially rotating cylinder is no longer antisymmetric about the cylinder mid-depth.

The predictions of Venezian's model describe the qualitative nature of the transient flows in a differentially rotating cylinder. However, Venezian's analysis was intended to be only a model calculation. In addition to the highly approximate nature of the basic assumptions leading to the use of the final-state angular speed Ω , the inadequacies of the original Wedemeyer model, which were carried over to the Venezian model, pose serious difficulties (see Ref. 9). Furthermore, the role of the parameter Ω_T/Ω_B is not fully accounted for in the formulation.

Numerical Model

The numerical model employs a finite-difference form of the unsteady, axisymmetric incompressible Navier-Stokes equations. Written in cylindrical coordinates rotating with the angular velocity Ω , with respective relative velocity components (u, v', w) , these equations are

$$\frac{\partial u}{\partial t} = -\frac{1}{r} \frac{\partial}{\partial r} \frac{\partial}{\partial r} (ruu) - \frac{\partial}{\partial z} (uw) + \frac{v'^2}{r} + 2\Omega v'$$

$$- \frac{1}{\rho} \frac{\partial p}{\partial r} + \nu \left[\frac{\partial}{\partial r} \frac{1}{r} \frac{\partial}{\partial r} (ru) + \frac{\partial^2 u}{\partial z^2} \right] \quad (3)$$

$$\frac{\partial v'}{\partial t} = -\frac{1}{r} \frac{\partial}{\partial r} (ruv') - \frac{\partial}{\partial z} (v'w) - \frac{v'u}{r}$$

$$- 2\Omega u + \nu \left[\frac{\partial}{\partial r} \frac{1}{r} \frac{\partial}{\partial r} (rv') + \frac{\partial^2 v'}{\partial z^2} \right] \quad (4)$$

$$\frac{\partial w}{\partial t} = -\frac{1}{r} \frac{\partial}{\partial r} (ruw) - \frac{\partial}{\partial z} (ww) - \frac{1}{\rho} \frac{\partial p}{\partial z}$$

$$+ \nu \left[\frac{1}{r} \frac{\partial}{\partial r} \left(r \frac{\partial w}{\partial r} \right) + \frac{\partial^2 w}{\partial z^2} \right] \quad (5)$$

Here p denotes the pressure (which includes the hydrostatic pressure and the centrifugal potential) and ρ the density. Note

that the azimuthal velocity v referred to in the inertial frame is related to v' through

$$v = v' + r\Omega$$

The continuity equation is

$$\frac{1}{r} \frac{\partial}{\partial r} (ru) + \frac{\partial w}{\partial z} = 0 \quad (6)$$

The initial conditions for the fluid are

$$u = w = 0, \quad v' = -r\Omega \quad \text{for } t = 0 \quad (7)$$

and the boundary conditions are

$$u = w = 0, \quad v' = r(\Omega_T - \Omega) \quad \text{at } z = H/2 \quad (8a)$$

$$u = w = 0, \quad v' = r(\Omega_B - \Omega) \quad \text{at } z = -H/2 \quad (8b)$$

$$u = w = 0, \quad v' = a(\Omega_S - \Omega) \quad \text{at } r = a \quad (8c)$$

To satisfy numerical stability requirements, the boundary conditions at the central axis are applied at a small, but finite radius ($r=r_i$),

$$u = 0, \quad v' = -r_i\Omega, \quad \partial w / \partial r = 0 \quad \text{for } r = r_i \quad (9)$$

Equations (3-6) and the initial and boundary conditions were finite differenced on a staggered mesh. To resolve the thin Ekman boundary layers [of thickness $\mathcal{O}(E^{1/2}H)$] near the end-wall disks, the grid was stretched in the z direction. The grid spacing was uniform in the r direction to have adequate resolution of the moving front [of thickness $\mathcal{O}(E^{1/2}H)$] in the interior. The pressure was found from the Poisson equation obtained by taking the divergence of Eqs. (3) and (5). The Poisson equation was solved by an ADI iterative approach. For further details on the numerical techniques, the reader is referred to Ref. 12.

The numerical model adopted was verified previously for quasilinear homogeneous spin-up flows¹² and for quasilinear stratified spin-up flows.¹⁴ These verifications were made by checking the model predictions against accurate rotating laser

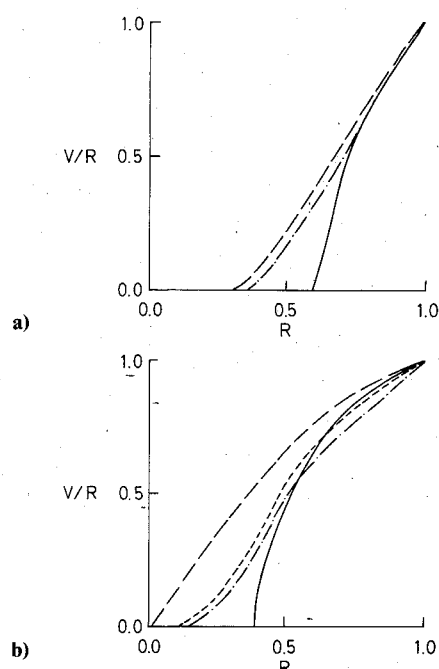


Fig. 1 Azimuthal velocity profiles: — case C1; --- case C2; — Wedemeyer-Venezian solution; times T are a) 0.51, b) 0.93.

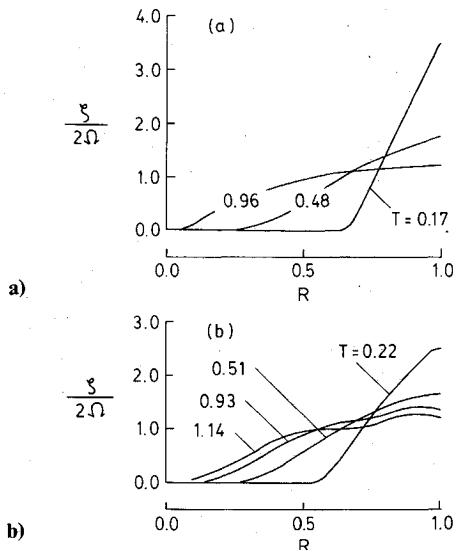


Fig. 2 Axial vorticity profiles for various times: a) case C3, and b) case C1.

Doppler velocimeter (LDV) measurements. More recently, the results of this numerical model were checked against the LDV measurements for spin-up from rest in a rigid cylinder.¹⁰ Despite several small differences existing between the numerical simulation and the laboratory experiment,¹² these comparisons exhibit excellent agreement, validating this numerical model for computing the transient flow details for various types of the spin-up process.

Results and Discussion

Numerical results have been obtained for spin-up from rest in a differentially rotating cylinder using three different sets of experimental parameters. All three cases were designed such that the final-state angular velocity prescribed by Venezian, $\Omega = [(\Omega_B^2 + \Omega_T^2)/2]^2$, has the same value, but that Ω_T/Ω_B has different values. The relevant fluid and geometrical parameters were modeled after the laboratory experiments of Hyun et al.¹⁰ as

$$a = 10.15 \text{ cm}, \quad H = 10.05 \text{ cm}, \quad \Omega = 0.211 \text{ rad/s}$$

$$\nu = 9.3 \times 10^{-3} \text{ cm}^2/\text{s}, \quad E[= \nu/\Omega H^2] = 4.36 \times 10^{-4}$$

As was pointed out by Venezian, the role of the sidewall is only secondary and the angular velocity of the sidewall does not affect the essential dynamics of the interior flow. For the sake of simplicity, therefore, we set $\Omega_S = \Omega$.

The values of Ω_T and Ω_B (units in rad/s) for the three cases are:

$$\text{C1, } \Omega_T = 0.145, \Omega_B = 0.289, \Omega_T/\Omega_B = 0.50$$

$$\text{C2, } \Omega_T = 0.182, \Omega_B = 0.242, \Omega_T/\Omega_B = 0.75$$

$$\text{C3, } \Omega_T = 0.211, \Omega_B = 0.211, \Omega_T/\Omega_B = 1.00$$

Obviously, case C3 corresponds to the spin-up from rest in a rigid cylinder.

The sensitivity of the results of this numerical model to grid size was tested by Warn-Varnas et al.¹² and Hyun et al.¹⁰ The present computations were performed using a 36×36 grid in the $(r-z)$ plane, which, due to the grid stretching, allowed approximately six grid points in the Ekman layer. The radius of the inner cylinder [see Eq. (9)] was set $r_i = 0.01$ cm; an increase of r_i to 0.1 cm produced no noticeable effect on the interior flow.¹² The time step was $\Delta t = 0.0125$ s, which assured accuracy and satisfied the computational stability

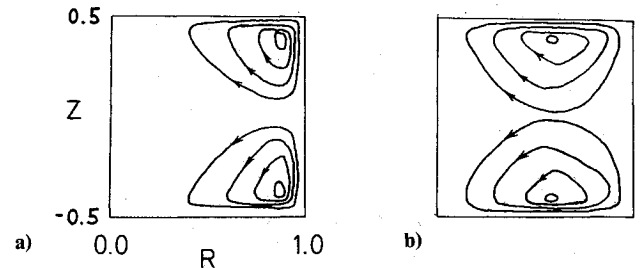


Fig. 3 Plots of the meridional stream function for case C3: a) at $T = 0.08$; $\psi_{\max} = 2.50$, $\psi_{\min} = 0.0$, the contour interval $\Delta\psi = 0.60$; b) at $T = 0.48$; $\psi_{\max} = 1.00$, $\psi_{\min} = 0.0$, $\Delta\psi = 0.30$ (units in cm^2/s).

criteria described by Warn-Varnas et al. For a complete set of parameters, the computer time required to integrate the equations up to $T \sim 1$ was approximately 5 h on a UNIVAC 1100 computer.

Azimuthal Flow

We note that the dominant flow is in the azimuthal direction and that the azimuthal velocity is vertically uniform in the interior for the small value of Ekman numbers considered here. Figure 1 shows the radial profile of the scaled nondimensional azimuthal velocity in the inertial frame V/R at two different times. For comparison purposes, the inviscid solution of the Wedemeyer-Venezian model [Eq. (2)] is also included. It is apparent in Fig. 1 that, as Ω_T/Ω_B becomes close to unity, the interior spins up faster and the propagation speed of the front increases. The discrepancy in the azimuthal flows between spin-up in a rigid cylinder ($\Omega_T/\Omega_B = 1$) and in a differentially rotating cylinder ($\Omega_T/\Omega_B \neq 1$) increases at large times. As anticipated, the predictions of the inviscid Wedemeyer-Venezian solution exhibit considerable departures from the numerical results, especially near the front.

The present numerical results indicate that the final-state is reached for $T \geq 2$ when the flowfields exhibit practically no variation with time (e.g., maximum changes in the flow variables are less than 1% over a period of $T \sim 0.1$). The numerical results also confirmed that the final-state angular speed of the fluid is quite satisfactorily described by the expression adopted by Venezian, $\Omega = [(\Omega_B^2 + \Omega_T^2)/2]^2$. Thus, the azimuthal velocity field in the final state can be given, to a high degree of accuracy, as $v = r\Omega$.

Axial Vorticity Field

An important field variable in the discussion of rotating fluid dynamics is the axial vorticity, $\xi = (1/r) [\partial(rv)/\partial r]$. Benton⁹ pointed out a serious inadequacy of the Wedemeyer model from the viewpoint of the axial vorticity field, despite the success of the model in describing the qualitative aspects of the flow. According to the Wedemeyer-Venezian model, the vorticity is zero in the region ahead of the front, and is nonzero but spatially uniform behind the front. (Figure 1 of Benton illustrates the vorticity distribution calculated according to Wedemeyer's solution.) The correct profiles of the axial vorticity had not been given previously.

Figure 2 shows the vorticity profiles computed by the present numerical solutions. For spin-up in a rigid cylinder (Fig. 2a for case C3) and in a differentially rotating cylinder (Fig. 2b for case C1), strong radial variations of the vorticity are noted behind the front, pointing to a substantial difficulty with the Wedemeyer-Venezian model. In general, the vorticity varies continuously from zero ahead of the front to a value larger than 2Ω behind the front. At early times, the vorticity behind the front overshoots the final-state value (2Ω) by an appreciable amount. As time progresses, the vorticity behind the front reduces to 2Ω from above. Figure 2 also shows that the adjustment of the vorticity to the final-state value is faster as the ratio Ω_T/Ω_B becomes close to unity. In summary, the

azimuthal velocity profiles indicate that spin-up proceeds more effectively as the ratio Ω_T/Ω_B becomes close to unity.

Meridional Flow

One of the most striking differences between spin-up in a rigid cylinder and in a differentially rotating cylinder is in the meridional flow. Here we define the axisymmetric stream function ψ such that $u = (1/r)(\partial\psi/\partial z)$, $w = -(1/r)(\partial\psi/\partial r)$. (Positive values of ψ imply counterclockwise meridional circulation.)

Figure 3 depicts typical plots of the meridional stream function in the meridional plane for spin-up in a rigid cylinder (case C3). Clearly, the meridional circulation is antisymmetric about the mid-depth plane $z=0$. These plots indicate that fluid in the interior is drawn into the Ekman layers ahead of the front, pushed radially outward in the Ekman layers, and then expelled to the interior behind the front. (Hyun et al.¹⁰ showed that the location of the front may be identified as the region where the magnitude of the radial velocity is greatest and the vertical velocity is very small.) The reversed meridional flow regions, which were observed to develop near the sidewall at early times,^{1,2} are not seen for case C3, presumably because of the relatively large value of $E [= \mathcal{O}(10^{-4})]$ used in the present calculations (see Kitchens^{1,2}). Figure 3 clearly indicates that, as time progresses, the

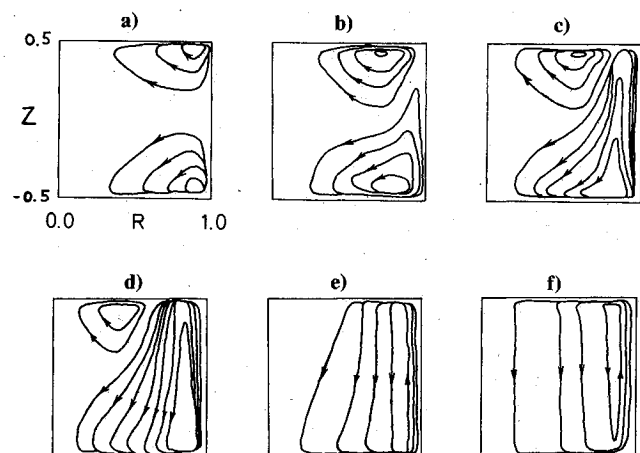


Fig. 4 Plots of the meridional stream function for case C1 (units in cm^2/s): a) at $T=0.05$; $\psi_{\max}=3.15$, $\psi_{\min}=-2.51$, $\Delta\psi=0.75$; b) at $T=0.24$; $\psi_{\max}=2.23$, $\psi_{\min}=-1.81$, $\Delta\psi=0.50$; c) at $T=0.50$; $\psi_{\max}=1.61$, $\psi_{\min}=-1.14$, $\Delta\psi=0.30$; d) at $T=0.97$; $\psi_{\max}=1.46$, $\psi_{\min}=-0.50$, $\Delta\psi=0.20$; e) at $T=1.37$; $\psi_{\max}=1.46$, $\psi_{\min}=-0.09$, $\Delta\psi=0.40$; f) at $T=1.96$; $\psi_{\max}=1.46$, $\psi_{\min}=0.00$, $\Delta\psi=0.40$.

meridional flow weakens (compare the values of ψ_{\max}), approaching the final state of a strictly solid-body rotation.

The meridional circulation patterns in a differentially rotating cylinder (case C1) are sketched in Fig. 4. At a very early time, the meridional flows are qualitatively similar to those arising in a rigid cylinder (see Figs. 3a and 4a). Note, however, that the meridional circulation is no longer strictly antisymmetric about the cylinder mid-depth. As time progresses, the deviation from the vertical antisymmetry about mid-depth is more pronounced. Since $\Omega_B > \Omega_T$ in the present calculations, the counterclockwise meridional circulation (driven by the faster-rotating bottom disk) is more rigorous and fills a larger portion of the meridional plane than the clockwise circulation (see Figs. 4a and 4b). At intermediate times (see Fig. 4c), the counterclockwise circulation penetrates up to the top disk. At large times, the clockwise circulation diminishes. Figures 4e and 4f illustrate the approach to the final state. Figure 4f depicts the final state when the meridional circulation in the interior consists of purely vertical flows sustained by the Ekman suction (blowing) at the faster (slower) rotating disk. Clearly, the return circuit is in the sidewall vertical boundary layer.

In order to gain further understanding of the meridional flow, the detailed profiles of the vertical velocity in the interior were examined. Figure 5 displays the profiles of the scaled vertical velocity, $W = w/(\nu\Omega)^{1/2}$, in the interior. The radial location is shown by separate curves on each graph. For spin-up in a rigid cylinder (see Fig. 5a for case C3), the vertical velocity is antisymmetric about mid-depth. The three curves in Fig. 5a are representative of the vertical velocity profiles in the interior regions ahead of, near, and behind the front, respectively. Ahead of the front, the vertical velocity is such that the interior fluid is drawn into the Ekman layers at both disks (see curve A). The vertical velocity is very small in the frontal region (e.g., curve B). Behind the front, the vertical velocity is such that the fluid is expelled from the Ekman layers into the interior (curve C).

In the case of spin-up in a differentially rotating cylinder, a qualitatively different picture emerges, as demonstrated in Figs. 5b and 5c, computed for case C2. At early times, the vertical velocity profiles are qualitatively similar to those in a rigid cylinder. Note, however, that the vertical velocity profiles are no longer strictly antisymmetric about the mid-depth (see Fig. 5b). At large times, the departure from vertical antisymmetry is more pronounced (see Fig. 5c). More significant is that at large times the blowing of the fluid into the interior behind the front is no longer present, i.e., the faster rotating disk sucks in the fluid in the interior behind the front as well as ahead of the front (compare curves C in Figs. 5b and 5c). This is clearly indicative of the approach to the

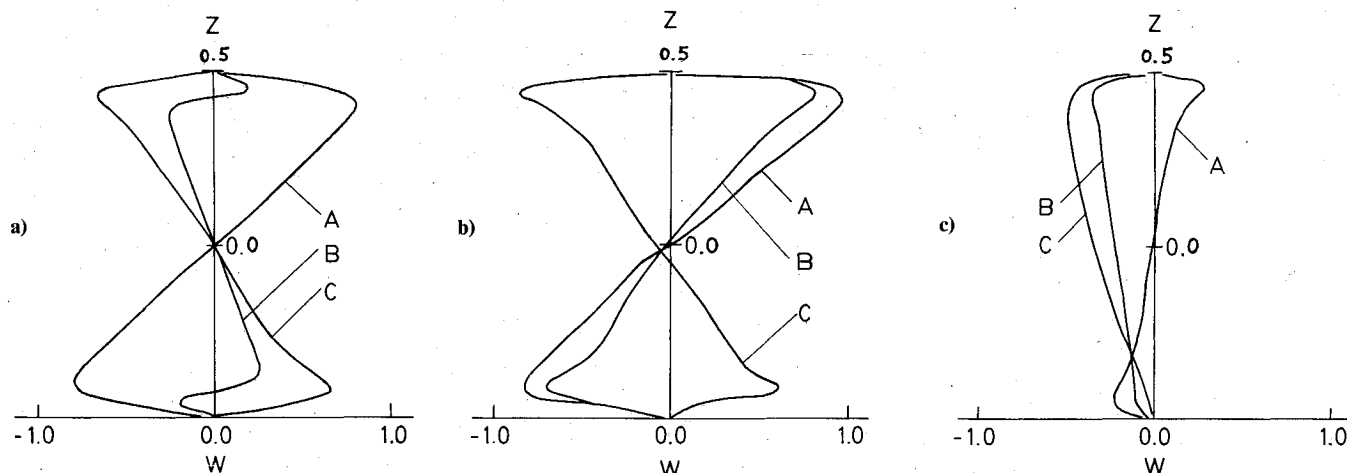


Fig. 5 Plots of the vertical velocity: a) for case C3 at $T=0.32$, the radial locations R of the curves are A) 0.40, B) 0.70, C) 0.80; b) for case C2 at $T=0.25$, the radial locations R of the curves are A) 0.40, B) 0.65, C) 0.82; c) same as in Fig. 5b except at $T=1.14$.

final state, when the meridional circulation is essentially made up of vertical flows pulled toward the faster rotating disk throughout the interior region.

Conclusion

Accurate and comprehensive flowfield data for spin-up from rest in a differentially rotating cylinder have been obtained by numerically integrating the unsteady Navier-Stokes equations. As Ω_T/Ω_B becomes close to unity, spin-up is generally more effective and the velocity shear front propagates faster. Unlike the predictions of the Wedemeyer-Venezian model, the axial vorticity varies continuously from zero ahead of the front to a value greater than 2Ω behind the front. The transient meridional circulation is not antisymmetric about the cylinder mid-depth as Ω_T/Ω_B deviates from unity. At large times, the faster rotating disk sucks in the interior fluid throughout its entire length. In the final state, the meridional circulation in the interior consists of purely vertical flows pulled toward the faster rotating disk.

Acknowledgments

Appreciation is extended to Dr. W.W. Fowles and Dr. F. Leslie of NASA Marshall Space Flight Center and Dr. A. Warn-Varnas of Naval Ocean Research and Development Activity. The computations were made at NASA Marshall Space Flight Center while the author was a visiting scientist. The visiting scientist appointment was supported by the Global Weather Program of the Office of Space Science and Applications, NASA Headquarters, Washington, D.C.

References

- ¹Kitchens, C. W. Jr., "Navier-Stokes Solutions for Spin-up from Rest in a Cylindrical Container," Ballistic Research Laboratory, Aberdeen Proving Ground, Md., ARBRL-TR-02193, Sept. 1979.
- ²Kitchens, C. W. Jr., "Navier-Stokes Solutions for Spin-up in a Filled Cylinder," *AIAA Journal*, Vol. 18, Aug. 1980, pp. 929-934.
- ³Kitchens, C. W. Jr., Gerber, N., and Sedney, R., "Spin Decay of Liquid-Filled Projectiles," *Journal of Spacecraft and Rockets*, Vol. 15, Nov.-Dec. 1978, pp. 348-354.
- ⁴Wedemeyer, E. H., "The Unsteady Flow within a Spinning Cylinder," *Journal of Fluid Mechanics*, Vol. 20, 1964, pp. 383-399.
- ⁵Venezian, G., "Spin-up of a Contained Fluid," *Topics in Ocean Engineering*, Vol. 1, 1969, pp. 212-223.
- ⁶Watkins, W. B. and Hussey, R. G., "Spin-up from Rest: Limitations of the Wedemeyer Model," *The Physics of Fluids*, Vol. 16, 1973, pp. 1530-1531.
- ⁷Watkins, W. B. and Hussey, R. G., "Spin-up from Rest in a Cylinder," *The Physics of Fluids*, Vol. 20, 1977, pp. 1596-1604.
- ⁸Weidman, P. D., "On the Spin-up and Spin-down of a Rotating Fluid, Pt. 1, Extending the Wedemeyer Model," *Journal of Fluid Mechanics*, Vol. 77, 1976, pp. 685-708.
- ⁹Benton, E. R., "Vorticity Dynamics in Spin-up from Rest," *The Physics of Fluids*, Vol. 22, 1979, pp. 1250-1251.
- ¹⁰Hyun, J. M., Leslie, F., Fowles, W. W., and Warn-Varnas, A., "Numerical Solutions for Spin-up from Rest in a Cylinder," *Journal of Fluid Mechanics*, Vol. 27, 1983, pp. 263-281.
- ¹¹Venezian, G., "Nonlinear Spin-up," *Topics in Ocean Engineering*, Vol. 2, 1970, pp. 87-96.
- ¹²Warn-Varnas, A., Fowles, W. W., Piacsek, S., and Lee, S. M., "Numerical Solutions and Laser Doppler Measurements of Spin-Up," *Journal of Fluid Mechanics*, Vol. 85, 1978, pp. 609-639.
- ¹³Greenspan, H. P., *The Theory of Rotating Fluids*, Cambridge University Press, Cambridge, England, 1968, p. 327.
- ¹⁴Hyun, J. M., Fowles, W. W., and Warn-Varnas, A., "Numerical Solutions for the Spin-up of a Stratified Fluid," *Journal of Fluid Mechanics*, Vol. 117, 1982, pp. 71-90.